MPMI Vol. 35, No. 6, 2022, pp. 477–487, https://doi.org/10.1094/MPMI-10-21-0247-R

e-Xtra*

Comparative Genomics of *Fusarium circinatum* Isolates Used to Screen Southern Pines for Pitch Canker Resistance

James C. Fulton,[1,†] Pei-Ling Yu,[1] Katherine E. Smith,[2,3] Jose C. Huguet-Tapia,[1] Owen Hudson,[1] April Meeks,[4] Tania Quesada,[2] Kathleen McKeever,[5] and Jeremy T. Brawner[1,†]

[1] Department of Plant Pathology, University of Florida, Gainesville, FL, U.S.A.
[2] School of Forest, Fisheries, and Geomatics Sciences, University of Florida, Gainesville, FL, U.S.A.
[3] United States Department of Agriculture Forest Service, Southern Institute of Forest Genetics, Saucier, MS, U.S.A.
[4] Rayonier, Andalusia, AL, U.S.A.
[5] United States Department of Agriculture Forest Service, Resistance Screening Center, Asheville, NC, U.S.A.

Accepted 6 March 2022.

Pitch canker, caused by the fungal pathogen *Fusarium circinatum*, is a global disease affecting many *Pinus* spp. Often fatal, this disease causes significant mortality in both commercially grown and natural pine forests and is an issue of current and growing concern. *F. circinatum* isolates collected from three locations in the U.S. state of Florida were shown to be virulent on both slash and loblolly pine, with two of the isolates causing equivalent and significantly larger lesions than those caused by the third isolate during pathogenicity trials. In addition, significant genetic variation in lesion length in the pedigreed slash pine population was evident and rankings of parents for lesion length were similar across isolates. Experimental data demonstrate that both host and pathogen genetics contribute to disease severity. High-quality genomic assemblies of all three isolates were created and compared for structural differences and gene content. No major structural differences were observed among the isolates; however, missing or altered genes do contribute to genomic variation in the pathogen population. This work evaluates in planta virulence among three isolates of *F. circinatum*, provides genomic resources to facilitate study of this organism, and details comparative genomic methods that may be used to explore the pathogen's contribution to disease development.

[†]Corresponding authors: J. C. Fulton; pcvgt@ufl.edu, and J. T. Brawner; jeremybrawner@ufl.edu

J. C. Fulton, P.-L. Yu, and K. E. Smith contributed equally to this work.

Funding: United States Department of Agriculture–National Institute of Food and Agriculture Tactical Sciences for Agricultural Biosecurity Institute of Food and Agricultural Sciences McIntire-Stennis project 13117320 and McIntire-Stennis grant number FLA-PLP-005931, "Developing and scaling up the next generation of healthy forests."

*The *e*-Xtra logo stands for "electronic extra" and indicates that supplementary tables and supplementary figures are published online.

The author(s) declare no conflict of interest.

Keywords: comparative genomics, effectors, fungal effectors, fungus–plant interactions, genomics, proteomics, mechanisms of pathogenicity, metabolomics, secondary metabolism

Pitch canker, caused by the fungal pathogen *Fusarium circinatum*, affects a wide range of pine species as well as Douglas-fir (*Pseudotsuga menziesii*) (Wingfield et al. 2008). Although believed to have originated in the Mesoamerican center of pine diversity, it has become a commonly reported disease of pine trees in the southeastern United States since being first reported in the United States in 1946 (Wikler and Gordon 2000). In the United States, the disease has been particularly damaging in slash pine (*Pinus elliottii*) and radiata pine (*P. radiata*) forests (Gordon et al. 2006).

Over the past 20 years, pitch canker has also become a problem in various countries where North American pine trees are cultivated as exotic plants (Drenkhan et al. 2020). *P. patula* forests in South Africa are being replanted with pitch-canker-resistant hybrid pine trees (Mitchell et al. 2012) and the disease is affecting the *P. radiata* nurseries and forests in California, Chile, Spain, and France (Martínez-Álvarez et al. 2014). The importance of the pathogen to the forest industry in South Africa led to the creation of the first fungal genome sequence from Africa (Wingfield et al. 2012). Stakeholders in the southeastern U.S. forest industry have expressed concern over the increased incidence of pitch canker as the disease has become more prevalent due to more intensive silvicultural techniques, including fertilization (personal communication), which is positively correlated with increased pitch canker severity (Fisher et al. 1981).

In southern pine trees, trees infected by the pathogen often develop symptoms such as copious resin exudation from lesions on stems, branches, or cones (Dwinell et al. 1985). Dead branches with white resin staining are the most frequently observed symptoms and this "flagging" is particularly evident following storm or hurricane damage to stands (Bezos et al. 2017; European Food Safety Authority (EFSA) et al. 2020). The disease is controlled by fungicides in nurseries where the pathogen can cause extensive seedling mortality (Gordon et al. 2015). Following establishment, losses from pitch-canker-induced mortality are readily observable; however, subsequent impacts on growth are not well quantified (Mitchell et al. 2011). The development of symptoms at midrotation following investments in weed control, fertilization, and thinning is particularly problematic where lesions on the

main stem often lead to defects that result in the downgrade of sawlogs into pulpwood and significant yield losses at harvest (Steenkamp et al. 2012).

Although *F. circinatum* was initially known only as a necrotrophic, wound-infecting pathogen of coniferous trees, recent research has revealed that an isolate of this fungus that kills shoot tissue when inoculated into a wound can also have a biotrophic relationship with roots of pine seedlings, infect and grow within grasses without causing symptoms, and cause ear rot of corn (Gordon and Reynolds 2017). *Fusarium* spp. synthesize a large array of mycotoxins in response to environmental stress as well as during the necrotrophic stage of infection (Perincherry et al. 2019). The categorization of fungal mycotoxins by chemical structure (lactones and terpenes), biosynthetic method (polyketides and amino acids), or species that produce them (*F. graminearum* and *F. culmorum*) (Munkvold 2017) reflects their diversity (Ji et al. 2019). Along with secreted cellulolytic enzymes and other effectors, mycotoxins hijack host secondary metabolism to steal host nutrients, kill host cells, and establish fungal growth, leading to the observed disease symptoms (Keller 2019). Mycotoxins are also targets of host defenses and are known to be involved in host selection and disease severity (Venkatesh and Keller 2019). Fungal genomes contain clusters of genes involved in toxin synthesis, transport, and regulation of cluster gene expression (Keller et al. 2005). These toxin clusters create an important source of diversity for fungi to draw upon in the face of changing environments such as climate, host genotype, and availability, which makes them an important line of inquiry for understanding virulence differences between isolates (Brakhage 2013).

Using methods developed by the United States Department of Agriculture (USDA) Forest Service Resistance Screening Center (RSC), differences in damage following inoculation with the pathogen have been reported in loblolly pine families (Kayihan et al. 2005) and populations of other pine species (Hodge and Dvorak 2007). This study presents data from an evaluation of the pathogenicity of three different isolates of *F. circinatum* following inoculation of pedigreed loblolly and slash pine populations. Clear differences in lesion length caused by the isolates prompted a characterization and analysis of genomic differences that may contribute to this phenotypic variation. This study provides reference quality genomes for three unique isolates that produced distinct phenotypes in a disease screening trial and bioinformatically identifies differences in genome composition and structure that may contribute to this phenotypic variability.

RESULTS

Evaluation of pathogenicity.

When slash and loblolly pine seedlings were inoculated with the Union County (Lake Butler), FL (LB) isolate of *F. circinatum*, the percentage of the stem that was damaged was significantly smaller ($P < 0.01$) than when the isolates from Volusia (VO) or Suwannee (SU) Counties were used for inoculation (Fig. 1). This result was repeated in both species in both runs of the experiment. The percentage of the stem that was damaged was greater in slash pine than it was in loblolly pine, with a mean and standard error of 9.6 ± 0.14% and 5.1 ± 0.17%, respectively. Differences among isolates were greater among slash pine families (LB = 3.1 ± 0.12%, SU = 11.4 ± 0.24%, and VO = 14.9 ± 0.26%) than in loblolly pine (LB = 0.6 ± 0.08%, SU = 8.1 ± 0.34%, and VO = 6.7 ± 0.31%). Although the differences between the VO and SU isolates were insignificant, seedlings inoculated with LB produced significantly smaller lesions ($P > 0.01$) in both slash and loblolly pine. Analysis of variance (ANOVA) results for slash and loblolly pine are provided in Tables 1 and 2.

Heritability estimates across all three isolates (0.25 ± 0.05) indicated that there is a significant level of genetic variance among the evaluated slash pine. Extended variance component models provided isolate specific estimates of heritability (LB = 0.29 ± 0.07, SU = 0.42 ± 0.06, and VO = 0.29 ± 0.06). The rankings of families across isolates were stable, as shown by an among-isolate genetic correlation of 0.85 ± 0.04. In contrast, the pooled heritability estimate from the loblolly pine experiment provided no evidence of genetic variation among families (narrow-sense heritability [h^2] was not statistically different than the null hypothesis) and isolate-specific heritability estimates indicated that the lack of damage caused by the LB isolate reduced the overall heritability estimate (LB = 0 ± 0, SU = 0.10 ± 0.06, and VO = 0.04 ± 0.05). Nevertheless, none of the heritability estimates for loblolly pine were significantly different than zero. Type-b correlation estimates indicated that family rankings did not change among isolates; however, the standard error of the correlation estimate indicated that the correlation was poorly estimated for loblolly pine (1.0 ± 0.61). ANOVA (Tables 1 and 2) and comparisons among family means for slash (10.0 ± 3.8%) and loblolly (4.4 and 1.7%) provide further support for underlying genetic differences contributing to phenotypic variation.

Genomic analysis.

Structural characteristics. Assembly statistics of the three inoculated *F. circinatum* genomes are presented in Table 3. Assembly sizes ranged from 46.2 Mb in the LB isolate to 47.9 Mb in the VO isolate. The size average was 47.1 Mb, slightly higher than the *F. circinatum* reference strain FSP 34 size of 44.0 Mb. Nanopore sequencing coverage ranged from 31 to 84×. GC content was consistent, with a small range from 46.8 to 47.0%. The N_{50} for scaffolded assemblies was as high as 4.14 Mb in LB and as low as 3.18 Mb in VO. Repeat sequence elements were 6.04% of the genome in SU, 6.79% in LB, and 7.52% in VO. The benchmarking universal single-copy ortholog (BUSCO) completeness scores for all de novo assemblies were greater than or equal to 99.6%.

Syntenic analysis of the SU assembly aligned to the reference *F. circinatum* isolate FSP 34 indicated that all SU chromosomes except for chromosome 11 were highly syntenic (≥82.8%) with corresponding chromosomes in the FSP 34 genome (Table 4). A translocation appeared to have redistributed a portion of chromosome 11 (58.3% synteny) to chromosome 8 (Fig. 2A). In other words, SU chromosome 8 appeared to contain a genomic portion that matched a region in FSP 34 chromosome 11. This perhaps explains the lower degree of synteny between chromosome 11 on SU and the FSP 34 isolate. When assembly scaffolds for LB and VO were aligned to the SU scaffolded assembly, there was a similarly high degree of overall synteny (≥81.7%) between these genomes and SU (Table 5). However, synteny of chromosome 10 in LB was very low (4.2%) while chromosome 11 in VO was modestly low (65.6%). It appears likely that chromosome 14 of the LB isolate is, in fact, a misscaffold placed on chromosome 10 (Fig. 2B). For example, chromosome 10 of SU is 2,675,794 bp long compared with LB's 124,851 bp. There is strong alignment between LB's chromosome 14 and SU's chromosome 10. Additional evidence is that LB's chromosome 14 is 2.6 Mbp long.

The percentage of chromosomal repeat induced point (RIP) mutation activity was similar to levels previously reported, with notable increases on chromosome 12 (van Wyk et al. 2019b). LB's chromosome 10 has 0 RIP mutation activity and is only 124,851 bp, likely due to utg12 not aligning to the NCBI reference or the SU isolate assembly. The percentage of the 2.6-Mb unaligned unitig12 of LB affected by RIP mutation was 11.4%, very similar to levels for chromosome 10 in the other genomes (Fig. 3).

Gene content. The number of annotated proteins was similar among the three genomes, with 15,703, 16,009, and 16,215 in

LB, SU, and VO, respectively. Approximately 9.5% of the proteins contained a signal peptide, 8% contained a signal peptide and no transmembrane domain, and approximately 1.8% were annotated as effectors in all genomes.

Evolutionary proximity between isolates was assessed by identifying orthologous genes present only as a single copy and applying a maximum-likelihood method to create a phylogenetic tree (Fig. 4). In summary, 48 single-copy genes were used with their own unique substitution model that allowed for distinct mutation rates per amino acid site as input into the tree. After 1,500 bootstrap replications, the log-likelihood of the tree was −7496285. The four de novo *F. circinatum* assemblies were located in one clade along with *F. circinatum* isolate FSP 34. These, together with *F. verticillioides* strain 7600, constituted a sister clade to the one encompassing *F. oxysporum* and *F. odoratissimum*. *F. proliferatum* and *F. fujikuroi* were more distantly related; however, there were less than an average of 0.03 amino acid substitutions per site, indicating a close genetic relationship. To further demonstrate the relationship of described isolates, UpSet and Venn diagram plots were used to display the distribution of identified orthologs (Fig. 5). There were 26 orthologous gene clusters that were unique to the *F. circinatum* isolates LB, S, and V, and there were 858 gene clusters shared among all *F. circinatum* isolates.

Effector and secondary metabolite analysis. To identify candidate proteins involved in mechanisms that led to the smaller lesion lengths observed in the LB isolate, we identified 295 orthologous gene clusters, consisting of 2,119 genes, missing in the LB isolate but present in both the SU and the VO isolates (Supplementary Table S1). We functionally annotated 340 genes from the SU isolate and 329 genes from the VO isolate. In all, 40 contained a signal peptide and no transmembrane domain, and 10 of those were identified as effectors by EffectorP. Of the 295 missing protein clusters, 130 were *F. circinatum* lineage specific and present only in the four *F. circinatum* isolates that were included in the analysis. The lineage-specific set included 10 genes annotated as transcription factors, including 2 that regulate biosynthesis of a secondary metabolite, 3 involved in polyketide synthesis, and 3 encoding secreted effectors that are involved in cell wall degradation.

Separately, antiSMASH was used to predict biosynthetic gene clusters in the de novo genome assemblies (Table 6). According to antiSMASH, only two metabolites, beauvericin and depudecin, were absent in LB yet present in SO and VU. Additionally, cyclosporin C was apparently present in LB yet absent in SO and VU. Primers (Supplementary Table S2) designed to amplify the missing portion of the depudecin synthase gene were used to confirm the bioinformatics result (Supplementary Fig. S2).

Carbohydrate-active enzyme annotation and distribution. Plant-pathogenic fungi secrete enzymes that modify polysaccharides (e.g., cellulose, hemicellulose, and pectin) of their host plant's cell wall in order to colonize their hosts and consume available carbon sources (Kubicek et al. 2014; Lombard et al. 2014). Therefore, the carbohydrate-active enzymes (CAZymes) produced by each of the isolates were compared to evaluate whether the lower virulence in LB was correlated with any of these components. The genomes of SU, LB, and VO contain 644, 646, and 641 genes encoding CAZymes, respectively (Table 7). Among these genes, 127, 127, and 128 were identified in the genomes of SU, LB, and VO, respectively, which encode plant cell-wall-degrading enzymes (Supplementary Table S3). Components of CAZymes associated with plant cell wall degradation are similar between all three isolates but glycoside hydrolase family 39 (GH39), which acts on hemicellulose, was only identified in

Table 1. Analysis of variance of percent damaged stem for loblolly pine

Variable	Sum Sq	Mean Sq	NumDF	DenDF	*F* value	*Pr* (> *F*)
Run	0.05574	0.05574	1	54.84	13.77	<0.01
Inoculum	1.628	0.81400	2	55.90	201.1	<0.01
Family	1.643	0.08646	19	55.08	21.36	<0.01
Run × Inoculum	0.06478	0.03239	2	54.84	8.003	<0.01
Family × Inoculum	0.7119	0.01873	38	55.08	4.629	<0.01

Table 2. Analysis of variance of percent damaged stem for slash pine

Variable	Sum Sq	Mean Sq	NumDF	DenDF	*F* value	*Pr* (> *F*)
Run	0.05473	0.05473	1	143.9	7.775	<0.01
Inoculum	5.217	2.608	2	150.8	370.5	<0.01
Family	2.758	0.04449	62	150.3	6.32	<0.01
Run × Inoculum	0.02465	0.01233	2	143.9	1.751	0.1773
Family × Inoculum	1.285	0.01147	112	144.5	1.63	<0.01

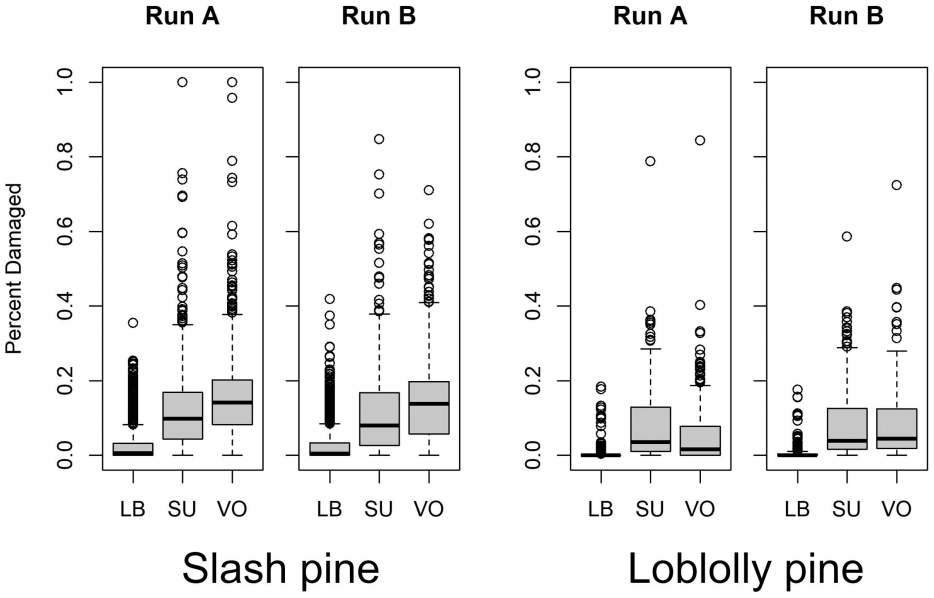

Fig. 1. Comparisons of the percentage of stem damaged following inoculation of slash and loblolly pine seedlings with three isolates of *Fusarium circinatum*. Data points are for individual trees and are intended to show the entire distribution of lesion length sizes. Lesion lengths were statistically different between Lake Butler (LB) versus Suwanee (SU) and Volusia (VO) isolates on both slash and loblolly pine.

VO (Supplementary Table S3). In general, the distribution of CAZymes is similar within these isolates and does not reveal any differences, which may explain the lower virulence of LB.

DISCUSSION

Significant genetic variation has been detected in southern pine populations, parents, and clones assessed for disease progression following inoculation with *F. circinatum* (Blakeslee et al. 1980; Gordon 2006; Kayihan et al. 2005; Quesada et al. 2010). ANOVA and significant heritability estimates in this study have provided further evidence that a systematic screening of pedigreed breeding populations may be used to identify individuals producing seedlings that have smaller lesions following inoculation. Assuming lesion length is associated with pitch canker resistance, the screening may be used to identify pine populations for reforestation in areas where the risk of pitch canker damage is high. Heritability estimates support the finding of significant differences among slash pine families ($h^2 = 0.25$) and indicate that the differences among loblolly are slight with h^2 estimates no different than zero. Genetic variation in the pathogen population was also observed, with significant differences among isolates supporting similar findings from previous studies (Quesada et al. 2019).

An understanding of differences in resistance among pine parents and differences in virulence of geographically distinct pathogen populations provides information useful for targeting where more resistant material should be planted. However, interactions among pine parents and *F. circinatum* isolates would greatly complicate the deployment of disease resistance across the landscape. The modified experimental design used for this study allowed for the detection of significant differences among hosts and pathogens as well as significant interactions ($P < 0.01$). Although the performance of some families changed significantly when different isolates were used, the rankings of slash pine families were generally stable when challenged with different isolates of the pathogen, as indicated by the genetic correlation of family rankings across the three isolates ($r_g = 0.85 \pm 0.04$). Although the modified screening protocol allowed for comparisons among isolates, the objective of ranking families for resistance would be better served by bulking several isolates to ensure that each seedling is challenged with a virulent isolate. Genetic variation among families could not be detected when the LB isolate was used.

Table 3. Statistics of de novo genome assemblies for isolates Lake Butler, Suwannee, and Volusia

Statistics	Lake Butler	Suwannee	Volusia
Filtered read number	58,257	93,129	155,740
Total gigabases	1.32	3.6	2.46
Coverage (×)	31	84	58
Contig number	21	21	25
Assembly size (Mb)	46.2	47.2	47.9
Longest contig (bp)	5,596,676	6,423,316	5,494,832
Unaligned contigs			
Number	2[a]	1[b]	5[a]
Length (bp)	2,848,166	239,773	1,227,736
GC (%)	46.8	46.9	47.0
N_{50} (bp)	4,141,639	3,637,485	3,183,314
N_{90} (bp)	900,966	1,110,995	1,899,496
Complete BUSCOs (%)[c]	99.6	99.7	99.6
Duplicate BUSCOs	29/4,494	12/4,494	43/4,494
Fragmented BUSCOs	8/4,494	8/4,494	10/4,494
Repeat elements (%)	6.79	6.04	7.52
Number of encoded proteins	15,703	16,009	16,215
SIGNALP	1,499	1,507	1,507
EffectorP	282	279	289
Missing BUSCOs	10/4,494	9/4,494	12/4,494

[a] In relation to the aligned and scaffolded Suwannee isolate.
[b] In relation to FSP 34.
[c] BUSCOs = benchmarking universal single-copy orthologs.

Developing an understanding of the pathogen virulence factors underlying the change in pine family rankings will require alternative experimental designs that provide phenotypes from a larger and more diverse set of isolates as well as their genomic resources. Screening of many more sequenced isolates with sufficient genetic variation would allow for the association of lesion length phenotypes with genomic variants to provide a more refined filter to identify genes of interest for further study. The significant difference in lesion development phenotype among the isolates used in this experiment provided the impetus to develop a comparative genomics pipeline to identify genomic differences that may underly differences in virulence. Genomic differences between virulent and avirulent isolates were evident; however, functional studies will be required to confirm that phenotypic differences in disease development result from these differences.

The bioinformatic methodology used in this study comparing different isolates of the same pathogenic fungus can be used to select genetic factors that may play a role in virulence differences; in this case, lesion length. We used OrthoMCL to determine clusters of genes specific to *F. circinatum* and discovered 10 transcription factors and three lineage-specific effectors involved in cell wall degradation, including a feruloyl esterase C, known to contribute to lesion length in the apple tree canker pathosystem (Xu et al. 2018). Pathogenic fungi are known to regulate the action of cell-wall-degrading enzymes through transcription factors induced by the presence of their polymer targets (Aro et al. 2005), making transcription factors important candidates for further study.

Secondary metabolite synthesis occurs in pathogenic fungi through the action of gene clusters. These clusters vary between lineages of fungi and can contribute to host pathogenicity. We used antiSMASH to identify secondary metabolites that may be missing in the less virulent LB isolate and found two differences: the depudecin cluster and the beauvericin cluster (Table 6). Beauvericin has antifungal activity and could possibly supply a competitive growth advantage but would not contribute to lesion length. The depudecin mycotoxin is a histone deacetylase inhibitor and a known virulence factor that contributes weakly to lesion diameter on cabbage leaves infected with *Alternaria brassicicola* (Wight et al. 2009). The *Fusarium* genus obtained the depudecin gene cluster by horizontal gene transfer, and subsequent gene loss and pseudogenization has led to cluster diversity (Reynolds et al. 2017). Differences between *F. circinatum* isolates' depudecin gene clusters could be at least partially responsible for differences in lesion length (Supplementary Figs. S2 and S3). Next steps in this line of inquiry would include detailed annotation of the clusters along with high-performance liquid chromatography analysis for the depudecin toxin.

Table 4. Percent syntenic similarity between *Fusarium circinatum* isolate FSP 34 and *F. circinatum* isolate Suwannee[a]

Chr (FSP 34)	Length in FSP 34 (bp)	Chr (Suwannee)	Synteny (%)
1	6,191,809	1	95.2017
2	4,774,899	2	96.3622
3	4,758,267	3	96.6759
4	4,141,359	4	87.8904
5	4,400,171	5	92.1849
6	4,055,048	6	95.0833
7	3,473,953	7	94.1859
8	3,085,006	8	82.8132
9	2,773,753	9	87.9313
10	2,372,785	10	89.0548
11	2,064,197	11	58.3079
12	526,391	12	92.038
Whole genome	42,617,638	–	87.9486

[a] Chr = chromosome.

In this current research, we reported three long-read genome assemblies of *F. circinatum*, expanding the genomic resources publicly available by nearly 50%. Our genomic assemblies are highly similar to reference isolate FSP 34 in both genetic content and organization. We have also identified potential virulence or pathogenic genes, including transcription factors, lineage-specific effectors, and a depudecin biosynthetic gene cluster whose absence may be associated with low virulence in LB using a comparative genomics approach. Despite that, further functional characterizations and expression analyses of candidate genes are required to elucidate their roles in the infection of *Pinus* spp. with *F. circinatum*.

MATERIALS AND METHODS

Isolate collection.

Isolates used in pathogenicity testing and comparative genomics studies were originally collected from naturally infected loblolly and slash pine trees in Volusia, Suwannee, and Union (Lake Butler) Counties, FL between 2016 and 2017, as described by Quesada et al. (2019). For long-term storage, the isolates were grown on sterile filter paper for 10 to 15 days, after which the filter paper was cut into small "confetti" (approximately 0.5-by-0.5-cm squares) and dried under the flow hood for 2 h. The filter paper was then placed in glass vials and stored at 4°C at the University of Florida. Some of these isolates on filter paper were shipped to the USDA Forest Service RSC in 2018 for inoculation tests (Quesada et al. 2019) and to expand their isolate collection. Isolates were initiated on pentachloronitrobenzene media at the RSC and pathogenicity was verified by inoculating 3-month-old seedlings with an aqueous spore suspension. Each genotype was reisolated from infected seedlings.

Inoculation and pathogenicity testing.

In 2019, 24 loblolly and 73 slash pine families were inoculated with the SU, VO, and LB isolates of *F. circinatum* at the RSC in Asheville, NC (Fig. 6A). The families were derived from cooperative tree improvement programs and represent deployment populations that are widely used for reforestation in the southeastern United States. A susceptible and a resistant seedlot were included in both the loblolly and slash pine disease screening experiments as controls. The RSC protocol requires that a set of 120 seedlings is artificially inoculated over 2 days in repeated assessments (namely, runs A and B) so that each family is represented by three trays in each run and each tray contains 20 seedlings. Suboptimal germination of some families resulted in fewer seedlings being available for the screening, with 7,560 of the 8,760 slash pine seedlings and 2,500 of the 2,880 loblolly pine seedlings being screened. Tolerance was assessed by applying an aqueous inoculum containing spores at a concentration of 100,000 spores/ml. This inoculum was sprayed directly onto a wound created by removing the top 1 to 2 cm of the seedling's leader to create an infection court. After 2 months, seedling height and lesion length (in millimeters) were measured to estimate the percentage of the stem that was damaged following inoculation (Young et al. 2006) (Fig. 6B). Lesion length and total seedling height were used to estimate the percentage of the stem damaged because this has been used to predict field performance following inoculation in different pine species (Gordon and Reynolds 2017).

Table 5. Percent syntenic similarity between all chromosomes of Suwannee (SU) and Lake Butler (LB) or Volusia (VO)[a]

Chr (SU)	Length in SU (bp)	Synteny (LB) (%)	Synteny (VO) (%)
1	6,423,316	93.6027	87.4944
2	5,355,507	91.9729	81.0215
3	5,723,900	78.5081	84.9671
4	4,387,587	85.3475	83.0157
5	4,508,281	87.7475	90.3456
6	4,511,134	75.535	85.5838
7	3,637,485	98.8508	87.5937
8	4,044,805	71.0452	70.6755
9	2,955,658	97.9479	91.6056
10	2,675,794	4.26382	93.6877
11	1,800,201	94.9525	65.6102
12	799,344	98.6438	90.9523
Genome	47,184,674	83.5836	81.6979

[a] Chr = chromosome.

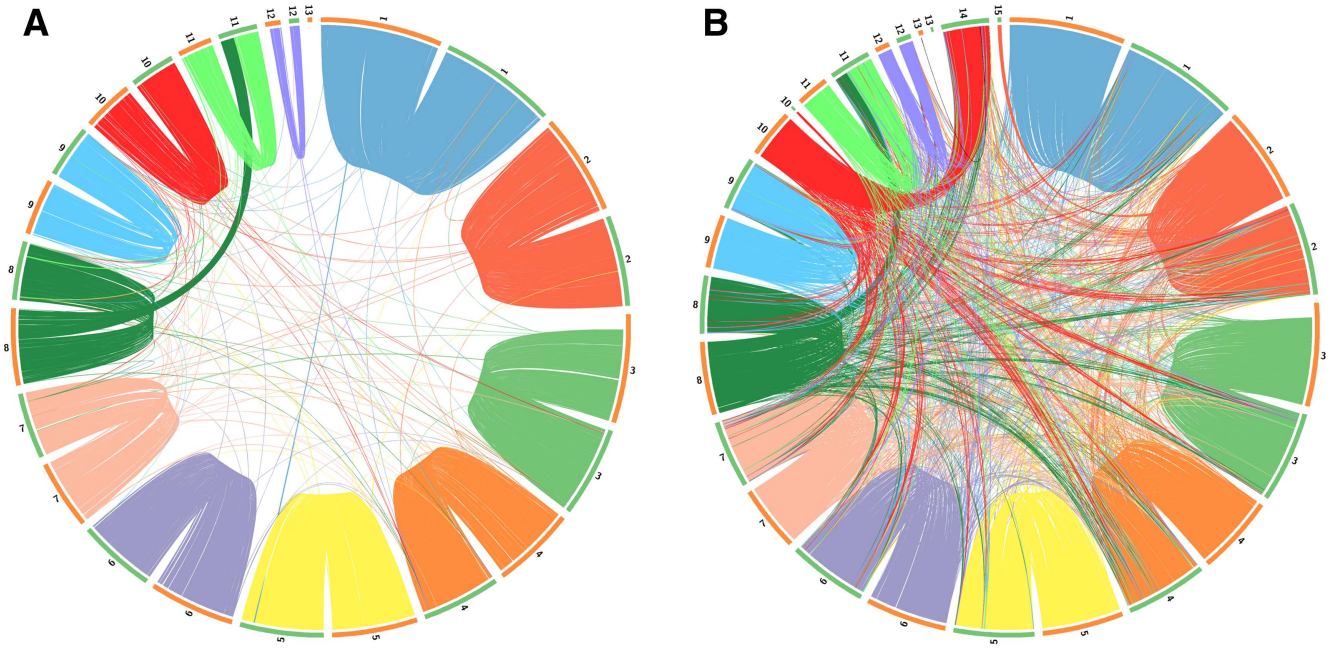

Fig. 2. Syntenic alignment among three *Fusarium circinatum* isolates (FSP 34, Suwannee, and Lake Butler) demonstrating the close overall similarity between each isolates' chromosomes. Chromosomes are represented by the green band for isolate **A,** FSP 34 and **B,** Lake Butler. Chromosomes of the Suwannee isolate are shown by the orange band in both. Locations of genomic alignments between chromosomes are shown by a colored link unique to each chromosome. For clarity, alignments less than 5 kb long are omitted.

Statistical analysis of pathogenicity.

A mixed linear model was tested which included as fixed effects the run, inoculum, control seedlots, and the run–inoculum interaction. The models included a random genetic effect associated with the additive relatedness matrix derived from pedigree and a random plot effect associated with differences among trays. Random effects were used to provide variance component estimates to infer the heritability of resistance traits following inoculation with the pathogen. The h^2 was estimated as the ratio of additive genetic variance to total variance as $h^2 = Va/(Va + Vp + Ve)$, where Va is the additive variance, Vp is the plot variance, and Ve is the error variance. The significance of changes in family rankings across the three different isolates was estimated using an extended variance component model that provided an estimate for a common type-b correlation (r_b) among breeding value predictions estimated for each of the isolates as well as isolate specific additive and error variances. Although inoculations were conducted using two species over 2 days and thousands of seedlings independently inoculated to evaluate differences between isolates, the experiment using all three isolates was not replicated in a subsequent evaluation; however, a subsequent study did reevaluate pathogenicity differences between the SU and LB isolates (Supplementary Fig. S1).

DNA extraction.

Isolates were grown on acidified potato dextrose agar (BD Difco, Detroit, MI, U.S.A.) overlaid with cellulose paper and incubated at 25°C for 5 days (Cassago et al. 2002). The mycelial mats were scraped from the cellulose and ground in liquid nitrogen. High-molecular-weight DNA was then extracted in cetyltrimethylammonium bromide (CTAB) extraction buffer (100 mM Tris-HCl [pH 9.5], 2% CTAB, 1.4 M NaCl, 1% PVP, 20 mM EDTA, and 0.25% b-mercaptoethanol [vol/vol]), using a modified version of the protocol described by Vaillancourt and Buell (2019). The Amicon buffer exchange step was eliminated, and genomic purification columns (Qiagen, Hilden, Germany) were used. To remove DNA molecules under 25 kb, a short-read eliminator kit (Circulomics, Inc., Baltimore, MD, U.S.A.) was used according to the manufacturer's instructions. DNA was analyzed for quality and

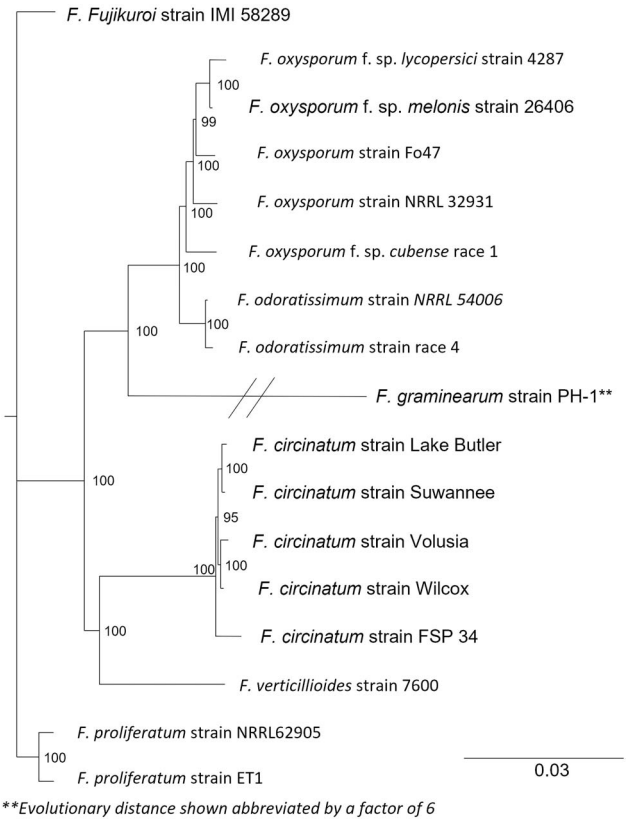

Fig. 4. Phylogenetic relationship of newly sequenced isolates Suwanee, Volusia, and Lake Butler in relation to their close genetic relatives. The evolutionary history was inferred by using a maximum-likelihood method using an edge-linked-proportional partition model with separate substitution models and separate rates across amino acid sites. The log-likelihood of the tree is −7496284.5580. Bootstrap values from 1,500 replications are shown next to tree branches. Trees are drawn to scale, with branch lengths measured in the number of substitutions per amino acid. In total, 48 single-copy orthologous genes from 17 organisms were included in the analysis. Although the tree is unrooted, the outgroup *Fusarium fujikuroi* is drawn at the root.

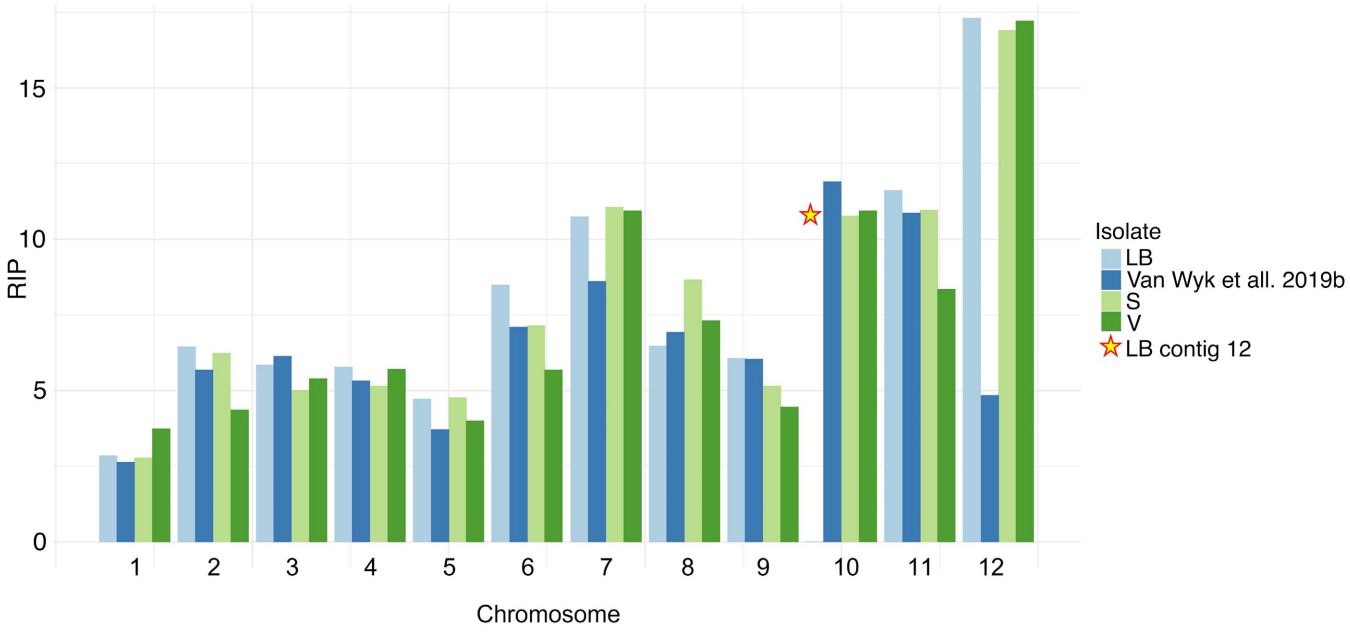

Fig. 3. Repeat-induced point (RIP) mutation activity across the chromosomes of isolates Lake Butler (+ utg12) (LB), Suwannee (S), Volusia (V), and van Wyk et al. (2019b).

size using a spectrophotometer and fluorometer (Thermo Fisher Scientific, Waltham, MA, U.S.A.) and electrophoresis (Agilent Technologies, Santa Clara, CA, U.S.A.).

Genomic sequencing, read processing, and quality control.

Libraries were prepared from 1.0 µg of quantified DNA using Oxford Nanopore Technology (ONT, Oxford, United Kingdom) ligation sequencing with native barcoding kits (SQK-LSK109, EXP-NBD104, and EXP-NBD114) according to the manufacturer's protocols. Prepared DNA was then sequenced on a FLO-MIN106 (R9.4) flow cell with the MinION platform for 72 h. Sequencing was monitored with ONT's MinKNOW v. 2.0. Raw signal data in FAST5 format was converted to basecalls using Guppy (v. 4.0.11) in high-accuracy mode. The resulting FASTQ files were concatenated into a single FASTQ file for each isolate. Reads were demultiplexed, and barcodes and adaptors were removed with Porechop (v.0.2.4). Reads were then filtered with Filtlong to exclude reads under 1,000 bp and read quality scores less than 14.3. Filtered reads were then visualized using Nanoplot (De Coster et al. 2018). Short-read genomic data produced by Illumina (San Diego, CA, U.S.A.) were previously described (Fulton et al. 2020).

De novo assembly.

Filtered ONT long reads were assembled into contigs using the SMARTdenovo assembler program. The Burrows-Wheeler Aligner (v.0.7.17) program indexed and aligned original Nanopore long-reads with the "-x ont2d" parameter selected (Li and Durbin 2009) back to the SMARTdenovo assembled contigs. The alignments generated were then used to error correct the SMARTdenovo assembled contigs using Racon (v.20161013) (Vaser et al. 2017). Next, the short-read sequences corresponding to each isolate were aligned to the Racon error-corrected long-read assemblies using Bowtie2 (v.2.4.2) (Langmead and Salzberg 2012; Langmead et al. 2019) and the alignments were used to polish the long-read assemblies using Pilon (v.1.22) (Walker et al. 2014). The Bowtie and Pilon steps were repeated until changes to the assemblies reached equilibrium. Ragtag (Alonge et al. 2019) was then used to align the assemblies to the reference *F. circinatum* strain FSP 39 genome (Table 8).

Table 6. Summary of predicted biosynthetic gene clusters with similarity to known clusters across all genomes

	Genomes[a]		
Clusters	**LB**	**SU**	**VO**
NRP			
Beauvericin	–	1	1
Cyclosporin C	1	–	–
NRP + polyketide			
Equisetin	1	1	1
Fusaridione A	1	1	1
Polyketide			
Oxyjavanicin	1	1	1
Fusaric acid	2	2	2
Bikaverin	1	1	1
(−)-Mellein	–	1	–
ACT-toxin II	1	1	–
Epipyriculol	1	1	–
Gibepyrone-A	1	1	1
Depudecin	–	1	1
Terpene			
Squalestatin S1	1	1	1
Gibberellin	1	1	1
Koraiol	1	1	1
α-Acorenol	1	1	1

[a] LB = Lake Butler, SU = Suwannee, and VO = Volusia.

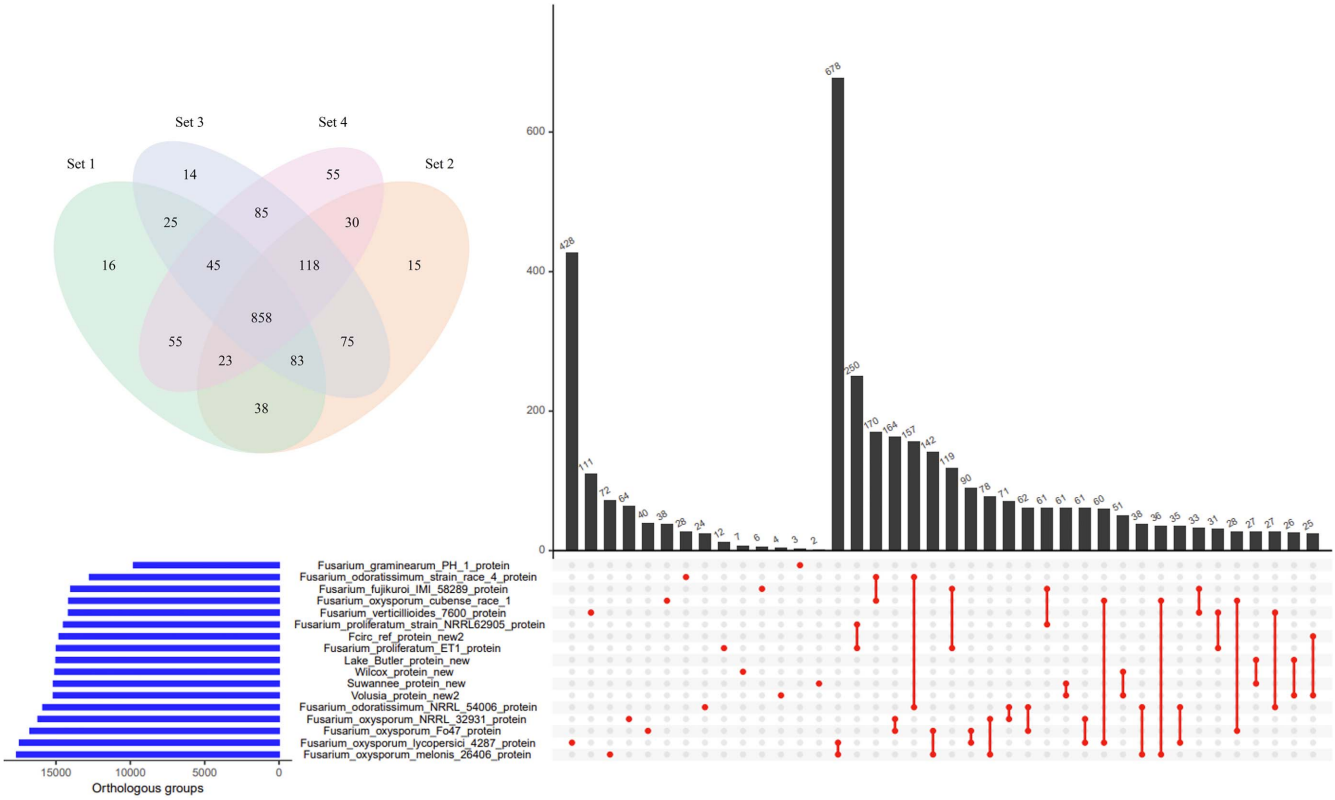

Fig. 5. Presence of identified single-copy orthologous gene clusters in *Fusarium* spp. An UpSet plot showing the distribution of single-copy orthologous gene clusters across several different species of *Fusarium*. The UpSet plot displays the number of distinct and overlapping orthologous gene clusters (vertical bars) in the *Fusarium* genomes. Inset: Venn diagram displaying only those orthologs present in at least one *Fusarium circinatum* isolate while entirely absent from other species. The listed sets are: Set 1, FSP 39; Set 2, Lake Butler; Set 3, Suwannee; and Set 4, Volusia.

Repetitive elements in each assembly were classified using RepeatModeler (v.2.0) (Smit et al. 2015) to generate custom repeat libraries. These repetitive element libraries were then used to create masked assemblies for annotation using RepeatMasker (v.4.1.1) (Smit et al. 2015). Statistics for the four long-read assemblies were assessed with BBmap (v.38.44) (Bushnell 2014) and the degree of completeness calculated using BUSCO (v.4.0.6) (Seppey et al. 2019). BUSCO training datasets included Eukaryota and Hypocreales.

Gene annotation.

MAKER (v.3.01.03) was used to annotate the assembled genomes (Cantarel et al. 2008). Transcript and protein evidence from *F. verticillioides* reference strain 7600 was used to model genes and the masked assemblies were used as genome input. An initial round of MAKER was run with the predicted genes used as input for training of SNAP (v.0.15.4) (Korf 2004). A second round of MAKER with the produced SNAP file was run and the predicted genes used as input for training of Augustus (v.3.3.2) (Stanke et al. 2006). A third round of MAKER was run, and the resulting gene predictions were used as a training set for GeneMark-ES (v.4.58) (Lukashin and Borodovsky 1998). Using the produced training datasets from SNAP, Augustus, and Genemark-ES, a final round of MAKER was run. Afterward, structural annotation was performed through a BLASTP (Altschul et al. 1997) homology search with an e-value threshold of 1e-5. Protein domains were annotated with InterProScan5 (v.5.35-74.0) (Jones et al. 2014). The Kyoto Encyclopedia of Genes and Genomes (KEGG) Automatic Annotation Server assigned KEGG identifiers to unique genes and proteins (Moriya et al. 2007).

Table 7. Comparison of plant cell-wall-degrading and fungal cell-wall-degrading carbohydrate-active enzyme (CAZyme) categories between different isolates[a]

Fungal isolates	GH	GT	PL	CE	CBM	AA	Total CAZyme modules
Reference	311	108	23	53	16	114	625
Suwanee	321	110	23	55	18	117	644
Lake Butler	320	112	23	55	18	118	646
Volusia	317	111	23	56	18	116	641

[a] Abbreviations: glycoside hydrolases (GH), glycoslyl transferases (GT), polysacccharide lyases (PL), carbohydrate esterases (CE), carbohydrate-binding modules (CBM), and auxiliary acticities (AA).

Orthologous gene families.

OrthoMCL (v.1.4) (Li et al. 2003) with a Blast *P* value cutoff of 1e-10 and a percent identity cutoff value of 60 was used to identify orthologous genes. Ortholog comparisons were made against *F. circinatum* strain FSP 39, *F. Fujikuroi* strain IMI 58289, *F. oxysporum* f. sp. *lycopersici* strain 4287, *F. oxysporum* f. sp. *melonis* strain 26406, *F. oxysporum* strain Fo47, *F. oxysporum* strain NRRL 32931, *F. oxysporum* f. sp. *cubense* race 1, *F. odoratissimum* strain *NRRL 54006, F. odoratissimum* strain race 4, *F. graminearum* strain PH-1, *F. verticillioides* strain 7600, *F. proliferatum* strain NRRL62905, and *F. proliferatum* strain ET1. After filtering, only orthologs present as a single copy in all genomes were kept in the dataset.

Phylogeny.

The remaining orthologs were aligned separately using MUSCLE (v.3.8.31) (Edgar 2004) with default parameters. The resulting alignments were trimmed with BMGE (v.1.12) (Criscuolo and Gribaldo 2010) and concatenated using FASconCAT-G (v.1.05) (Kück and Longo 2014). In all, 1,500 bootstrap replicates were completed using UFBoot2 (Hoang et al. 2018) in IQ-TREE (v.2.1.2) (Nguyen et al. 2015). The maximum-likelihood tree using an edge-linked proportional-partition model with separate substitution models and separate rates across amino acid sites was employed. The tree was constructed using 1,500 bootstrap replications and 48 partition models.

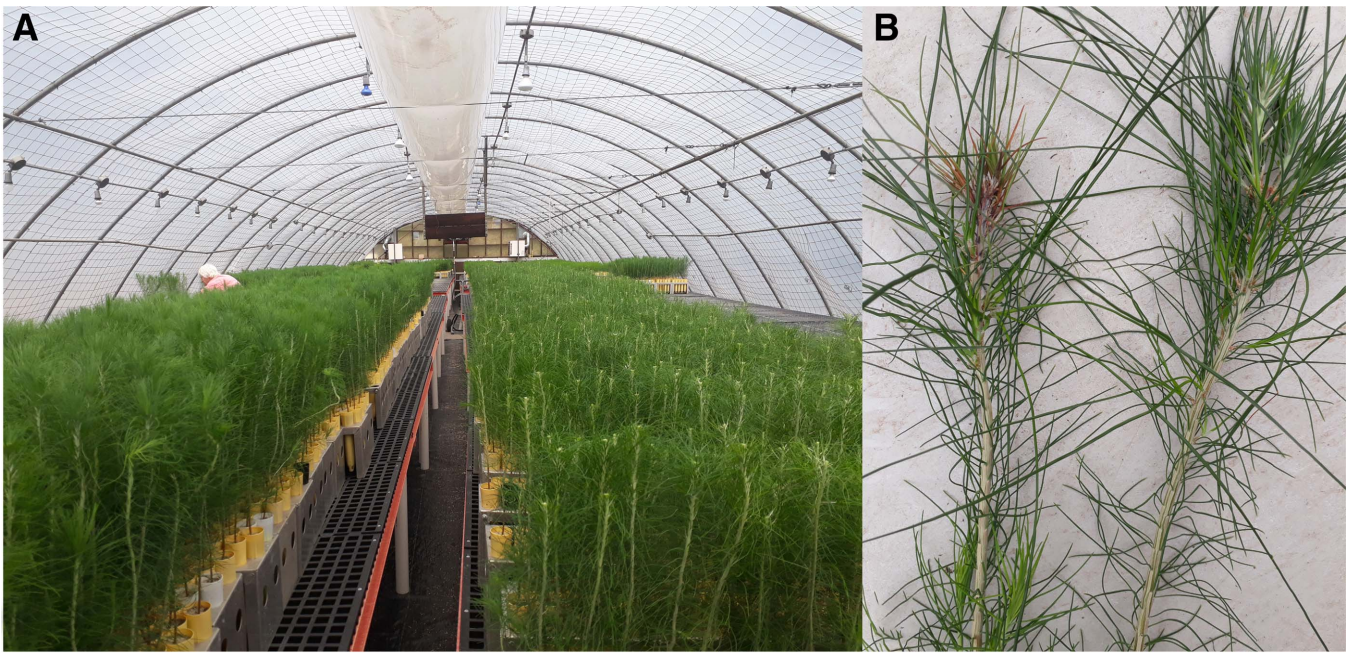

Fig. 6. Pathogenicity experiment to demonstrate variability of virulence among three isolates of *Fusarium circinatum*. **A,** In 2019, 24 loblolly and 73 slash pine families were inoculated with three different *F. circinatum* aqueous spore solutions at a concentration of 100,000 spores/ml. For each family, a set of 120 seedlings was artificially inoculated over 2 days. Each family was represented by three trays in each run and each tray contained 20 seedlings. A susceptible and a resistant seedlot were included in both the loblolly and slash pine disease screening experiments as controls. This inoculum was sprayed directly onto a wound created by removing the top 1 to 2 cm of the seedling's leader to create an infection court. **B,** After 2 months, seedling height and lesion length (in millimeters) were measured to estimate the percentage of the stem that was damaged by inoculation. The stem on the left (B) is infected (purple discoloration) while the stem on the right is healthy.

Table 8. Publicly available assemblies and protein datasets for which phylogenetic comparisons were conducted

Isolate	Host	Accession number	Reference
Fusarium fujikuroi strain IMI 58289	*Oryza sativa*	GCF_900079805.1	Wiemann et al. 2013
F. oxysporum f. sp. *melonis* strain 26406	*Cucumis melo*	GCA_002318975.1	Ma et al. 2014
F. verticilloides 7600	*Zea mays*	GCF_000149555.1	Gardiner 2018
F. graminearum strain PH 1	*Z. mays*	GCF_000240135.3	Walkowiak et al. 2016
F. circinatum FSP 34	*Pinus radiata*	GCA_000497325.3	Britz et al. 2001
F. oxysporum f. sp. *lycopersici* 4287 (race 2, VCG 0030)	*Solanum lycopersicum*	GCF_000149955.1	Ma et al. 2010
F. oxysporum strain Fo47	Endophyte; biocontrol agent	GCA_013085055.1	Wang et al. 2020
F. oxysporum f. sp. *cubense* race 1	*Musa acuminata* Cavendish subgroup	GCA_016802225.1	Maymon et al. 2020
F. odoratissimum strain NRRL 54006 (*F. oxysporum* f. sp. *cubense* tropical race 4 54006)	*M. acuminata* Cavendish subgroup	GCF_000260195.1	Ordonez et al. 2015
F. odoratissimum strain race 4 (*F. oxysporum* f. sp. *cubense* tropical race 4)	*M. acuminata* Cavendish Subgroup	GCA_000350365.1	Torres Bedoya et al. 2021
F. proliferatum strain NRRL62905	*Z. mays*	GCA_900029915.1	Munkvold et al. 1998
F. proliferatum strain ET1	Endophyte	GCF_900067095.1	Tsavkelova et al. 2008
F. oxysporum strain NRRL 32931	*Homo sapiens*	GCF_000271745.1	Zhang et al. 2020
F. circinatum strain Lake Butler	*P. elliottii*	GCA_013168825.2	This study; Fulton et al. 2020; Quesada et al. 2019
F. circinatum strain Suwannee	*P. elliottii*	GCA_013168835.2	This study; Fulton et al. 2020; Quesada et al. 2019
F. circinatum strain Volusia	*P. elliottii*	GCA_013168815.2	This study; Fulton et al. 2020; Quesada et al. 2019

Structural characteristic analyses.

The SU assembly was aligned to *F. circinatum* strain FSP 39 using Minimap2 (Li 2018) and the resulting aligned contigs scaffolded using Ragtag v. 1.0.0 (Alonge et al. 2019). Afterward, the LB and VO assemblies were aligned and scaffolded against the SU reference-aligned scaffold. Gaps between contigs were filled with 100 'N' characters. To assess synteny between scaffolded chromosomes, Satsuma2 was employed using default parameters (Grabherr et al. 2010). Circos (v.0.69-9) (Krzywinski et al. 2009) was used to visualize syntenic areas. Alignments greater or equal to 5,000 kb were depicted. Finally, RIP mutation analysis was done using the online tool RIPer (van Wyk et al. 2019a)

Effector and secondary metabolite analysis.

Annotated proteins from the three isolates were evaluated for effector and secondary metabolite production. Protein datasets were first screened for secretory signal peptides using Signal-P (v.5.0) (Almagro Armenteros et al. 2019). Afterward, only those proteins with attached signal peptides were used as input for EffectorP 2.0 (Sperschneider et al. 2016) to identify putative effectors. Secondary metabolites were discovered by application of the programs antiSMASH (antibiotics and secondary metabolite analysis shell; fungal version 6) (Blin et al. 2021) and dbCAN2 (automated CAZyme annotation) (Zhang et al. 2018). HMMER was used to search against the dbCAN HMMdb (release 9.0) (e-value < 1e-15, coverage > 0.35).

Data availability.

Genomes and sequence reads were deposited in the NCBI GenBank repository under BioProject number PRJNA757390. Accession numbers for all genomes used in the study are shown in Table 8.

AUTHOR-RECOMMENDED INTERNET RESOURCES

antiSMASH fungal version 6: https://fungismash.secondarymetabolites.org
dbCAN2: https://bcb.unl.edu/dbCAN2/index.php
Filtlong: https://github.com/rrwick/Filtlong/blob/main/README.md#faq
Porechop v.0.2.4: https://github.com/rrwick/Porechop
RIPper tool: https://theripper.hawk.rocks/#/home

LITERATURE CITED

Almagro Armenteros, J. J., Tsirigos, K. D., Sønderby, C. K., Petersen, T. N., Winther, O., Brunak, S., von Heijne, G., and Nielsen, H. 2019. SignalP 5.0 improves signal peptide predictions using deep neural networks. Nat. Biotechnol. 37:420-423.

Alonge, M., Soyk, S., Ramakrishnan, S., Wang, X., Goodwin, S., Sedlazeck, F. J., Lippman, Z. B., and Schatz, M. C. 2019. RaGOO: Fast and accurate reference-guided scaffolding of draft genomes. Genome Biol. 20:224.

Altschul, S. F., Madden, T. L., Schäffer, A. A., Zhang, J., Zhang, Z., Miller, W., and Lipman, D. J. 1997. Gapped BLAST and PSI-BLAST: A new generation of protein database search programs. Nucleic Acids Res. 25:3389-3402.

Aro, N., Pakula, T., and Penttilä, M. 2005. Transcriptional regulation of plant cell wall degradation by filamentous fungi. FEMS Microbiol. Rev. 29:719-739.

Bezos, D., Martinez-Alvarez, P., Fernandez, M., and Diez, J. J. 2017. Epidemiology and management of pine pitch canker disease in Europe—A review. Balt. For. 23:279-293.

Blakeslee, G. M., Dwinell, L. D., and Anderson, R. L. 1980. Pitch canker of southern pines: Identification and management considerations. United States Department of Agriculture Forest Service, Southeastern Area.

Blin, K., Shaw, S., Kloosterman, A. M., Charlop-Powers, Z., van Wezel, G. P., Medema, M. H., and Weber, T. 2021. antiSMASH 6.0: Improving cluster detection and comparison capabilities. Nucleic Acids Res. 49:W29-W35.

Brakhage, A. A. 2013. Regulation of fungal secondary metabolism. Nat. Rev. Microbiol. 11:21-32.

Britz, H., Couhnho, T., Gordon, T., and Wingfield, M. 2001. Characterisation of the pitch canker fungus, *Fusarium circinatum*, from Mexico. S. Afr. J. Bot. 67:609-614.

Bushnell, B. 2014. BBMap: A Fast, Accurate, Splice-Aware Aligner. Lawrence Berkeley National Lab, Berkeley, CA, U.S.A.

Cantarel, B. L., Korf, I., Robb, S. M., Parra, G., Ross, E., Moore, B., Holt, C., Sánchez Alvarado, A., and Yandell, M. 2008. MAKER: An easy-to-use annotation pipeline designed for emerging model organism genomes. Genome Res. 18:188-196.

Cassago, A., Panepucci, R., Baião, A., and Henrique-Silva, F. 2002. Cellophane based mini-prep method for DNA extraction from the filamentous fungus *Trichoderma reesei*. BMC Microbiol. 2:14.

Criscuolo, A., and Gribaldo, S. 2010. BMGE (Block Mapping And Gathering With Entropy): A new software for selection of phylogenetic informative regions from multiple sequence alignments. BMC Evol. Biol. 10:210.

De Coster, W., D'Hert, S., Schultz, D. T., Cruts, M., and Van Broeckhoven, C. 2018. NanoPack: Visualizing and processing long-read sequencing data. Bioinformatics 34:2666-2669.

Drenkhan, R., Ganley, B., Martín-García, J., Vahalík, P., Adamson, K., Adamčíková, K., Ahumada, R., Blank, L., Bragança, H., Capretti, P., Cleary, M., Cornejo, C., Davydenko, K., Diez, J. J., Lehtijärvi, H. T. D., Dvořák, M., Enderle, R., Fourie, G., Georgieva, M., Ghelardini, L., Hantula, J., Ioos, R., Iturritxa, E., Kanetis, L., Karpun, N. N., Koltay, A., Landeras, E., Markovskaja, S., Mesanza, N., Milenković, I., Musolin, D., Nilolaou, K., Nowakowska, J. A., Ogris, N., Oskay, F., Oszako, T., Papazova-Anakieva, I., Paraschiv, M., Pasquali, M., Pecori, F., Rafoss, T., Raitelaitytė, K., Raposo, R., Robin, C., Rodas, C. A., Santini, A., Sanz-Ros, A. V., Selikhovkin, A. V., Solla, A., Soukainen, M., Soulioti, N., Steenkamp, E. T., Tsopelas, P., Vemić, A., Vettraino, A. M., Wingfield, M. J., Woodward, S., Zamora-Ballesteros, C., and Mullet, M. S. 2020. Global geographic distribution and host range of *Fusarium circinatum*, the causal agent of pine pitch canker. Forests 11:724.

Dwinell, L. D., Barrows-Broaddus, J. B., and Kuhlman, E. G. 1985. Pitch canker: A disease complex. Plant Dis. 69:270-276.

Edgar, R. C. 2004. MUSCLE: Multiple sequence alignment with high accuracy and high throughput. Nucleic Acids Res. 32:1792-1797.

European Food Safety Authority (EFSA), Kinkar, M., and Vos, S. 2020. Pest survey card on *Fusarium circinatum*. EFSA Supporting Publ. 17: 1842E.

Fisher, R., Garbett, W., and Underhill, E. 1981. Effects of fertilization on healthy and pitch canker-infected pines. South. J. Appl. For. 5:77-79.

Fulton, J. C., Huguet-Tapia, J. C., Adams, S. M., Dufault, N. S., Quesada, T., and Brawner, J. T. 2020. Draft genome sequences of three *Fusarium circinatum* isolates used to inoculate a pedigreed population of *Pinus elliottii* seedlings. Microbiol. Resour. Announce. 9:e00631-20.

Gardiner, D. M. 2018. Genome sequences of three isolates of *Fusarium verticillioides*. Microbiol. Resour. Announce. 7:e00918-18.

Gordon, T. R. 2006. Pitch canker disease of pines. Phytopathology 96: 657-659.

Gordon, T. R., Kirkpatrick, S. C., Aegerter, B. J., Wood, D. L., and Storer, A. J. 2006. Susceptibility of Douglas fir (*Pseudotsuga menziesii*) to pitch canker, caused by *Gibberella circinata* (anamorph = *Fusarium circinatum*). Plant Pathol. 55:231-237.

Gordon, T. R., and Reynolds, G. J. 2017. Plasticity in plant-microbe interactions: A perspective based on the pitch canker pathosystem. Phytoparasitica 45:1-8.

Gordon, T. R., Swett, C. L., and Wingfield, M. J. 2015. Management of Fusarium diseases affecting conifers. Crop Prot. 73:28-39.

Grabherr, M. G., Russell, P., Meyer, M., Mauceli, E., Alföldi, J., Di Palma, F., and Lindblad-Toh, K. 2010. Genome-wide synteny through highly sensitive sequence alignment: Satsuma. Bioinformatics 26:1145-1151.

Hoang, D. T., Chernomor, O., von Haeseler, A., Minh, B. Q., and Vinh, L. S. 2018. UFBoot2: Improving the ultrafast bootstrap approximation. Mol. Biol. Evol. 35:518-522.

Hodge, G. R., and Dvorak, W. S. 2007. Variation in pitch canker resistance among provenances of *Pinus patula* and *Pinus tecunumanii* from Mexico and Central America. New For. 33:193-206.

Ji, F., He, D., Olaniran, A., Mokoena, M., Xu, J., and Shi, J. 2019. Occurrence, toxicity, production and detection of Fusarium mycotoxin: A review. Food Prod. Process. Nutr. 1:6.

Jones, P., Binns, D., Chang, H.-Y., Fraser, M., Li, W., McAnulla, C., McWilliam, H., Maslen, J., Mitchell, A., Nuka, G., Pesseat, S., Quinn, A. F., Sangrador-Vegas, A., Scheremetjew, M., Yong, S. Y., Lopez, R., and Hunter, S. 2014. InterProScan 5: Genome-scale protein function classification. Bioinformatics 30:1236-1240.

Kayihan, G. C., Huber, D. A., Morse, A. M., White, T. L., and Davis, J. M. 2005. Genetic dissection of fusiform rust and pitch canker disease traits in loblolly pine. Theor. Appl. Genet. 110:948-958.

Keller, N. P. 2019. Fungal secondary metabolism: Regulation, function and drug discovery. Nat. Rev. Microbiol. 17:167-180.

Keller, N. P., Turner, G., and Bennett, J. W. 2005. Fungal secondary metabolism—From biochemistry to genomics. Nat. Rev. Microbiol. 3: 937-947.

Korf, I. 2004. Gene finding in novel genomes. BMC Bioinf. 5:59.

Krzywinski, M., Schein, J., Birol, I., Connors, J., Gascoyne, R., Horsman, D., Jones, S. J., and Marra, M. A. 2009. Circos: An information aesthetic for comparative genomics. Genome Res. 19:1639-1645.

Kubicek, C. P., Starr, T. L., and Glass, N. L. 2014. Plant cell wall-degrading enzymes and their secretion in plant-pathogenic fungi. Annu. Rev. Phytopathol. 52:427-451.

Kück, P., and Longo, G. C. 2014. FASconCAT-G: Extensive functions for multiple sequence alignment preparations concerning phylogenetic studies. Front. Zool. 11:81.

Langmead, B., and Salzberg, S. L. 2012. Fast gapped-read alignment with Bowtie 2. Nat. Methods 9:357-359.

Langmead, B., Wilks, C., Antonescu, V., and Charles, R. 2019. Scaling read aligners to hundreds of threads on general-purpose processors. Bioinformatics 35:421-432.

Li, H. 2018. Minimap2: Pairwise alignment for nucleotide sequences. Bioinformatics 34:3094-3100.

Li, H., and Durbin, R. 2009. Fast and accurate short read alignment with Burrows–Wheeler transform. Bioinformatics 25:1754-1760.

Li, L., Stoeckert, C. J., Jr., and Roos, D. S. 2003. OrthoMCL: Identification of ortholog groups for eukaryotic genomes. Genome Res. 13: 2178-2189.

Liu, H., Wu, S., Li, A., and Ruan, J. SMARTdenovo: A de novo assembler using long noisy reads. Preprints 2020:2020090207.

Lombard, V., Golaconda Ramulu, H., Drula, E., Coutinho, P. M., and Henrissat, B. 2014. The carbohydrate-active enzymes database (CAZy) in 2013. Nucleic Acids Res. 42:D490-D495.

Lukashin, A. V., and Borodovsky, M. 1998. GeneMark.hmm: New solutions for gene finding. Nucleic Acids Res. 26:1107-1115.

Ma, L. J., Shea, T., Young, S., Zeng, Q., and Kistler, H. C. 2014. Genome sequence of *Fusarium oxysporum* f. sp. *melonis* strain NRRL 26406, a fungus causing wilt disease on melon. Genome Announce. 2: e00730-14.

Ma, L. J., van der Does, H. C., Borkovich, K. A., Coleman, J. J., Daboussi, M. J., Di Pietro, A., Dufresne, M., Freitag, M., Grabherr, M., Henrissat, B., Houterman, P. M., Kang, S., Shim, W. B., Woloshuk, C., Xie, X., Xu, J. R., Antoniw, J., Baker, S. E., Bluhm, B. H., Breakspear, A., Brown, D. W., Butchko, R. A., Chapman, S., Coulson, R., Coutinho, P. M., Danchin, E. G., Diener, A., Gale, L. R., Gardiner, D. M., Goff, S., Hammond-Kosack, K. E., Hilburn, K., Hua-Van, A., Jonkers, W., Kazan, K., Kodira, C. D., Koehrsen, M., Kumar, L., Lee, Y. H., Li, L., Manners, J. M., Miranda-Saavedra, D., Mukherjee, M., Park, G., Park, J., Park, S. Y., Proctor, R. H., Regev, A., Ruiz-Roldan, M. C., Sain, D., Sakthikumar, S., Sykes, S., Schwartz, D. C., Turgeon, B. G., Wapinski, I., Yoder, O., Young, S., Zeng, Q., Zhou, S., Galagan, J., Cuomo, C. A., Kistler, H. C., and Rep, M. 2010. Comparative genomics reveals mobile pathogenicity chromosomes in *Fusarium*. Nature 464:367-373.

Martínez-Álvarez, P., Pando, V., and Diez, J. 2014. Alternative species to replace Monterey pine plantations affected by pitch canker caused by *Fusarium circinatum* in northern S pain. Plant Pathol. 63:1086-1094.

Maymon, M., Sela, N., Shpatz, U., Galpaz, N., and Freeman, S. 2020. The origin and current situation of *Fusarium oxysporum* f. sp. *cubense* tropical race 4 in Israel and the Middle East. Sci. Rep. 10:1590.

Mitchell, R. G., Steenkamp, E. T., Coutinho, T. A., and Wingfield, M. J. 2011. The pitch canker fungus, *Fusarium circinatum*: Implications for South African forestry. South. For. J. For. Sci. 73:1-13.

Mitchell, R. G., Wingfield, M. J., Hodge, G., Steenkamp, E. T., and Coutinho, T. A. 2012. Selection of *Pinus* spp. in South Africa for tolerance to infection by the pitch canker fungus. New For. 43:473-489.

Moriya, Y., Itoh, M., Okuda, S., Yoshizawa, A. C., and Kanehisa, M. 2007. KAAS: An automatic genome annotation and pathway reconstruction server. Nucleic Acids Res. 35:W182-W185.

Munkvold, G., Stahr, H. M., Logrieco, A., Moretti, A., and Ritieni, A. 1998. Occurrence of fusaproliferin and beauvericin in *Fusarium*-contaminated livestock feed in Iowa. Appl. Environ. Microbiol. 64:3923-3926.

Munkvold, G. P. 2017. *Fusarium* species and their associated mycotoxins. Pages 51-106 in: Mycotoxigenic Fungi. A. Moretti and A. Susca, eds. Methods in Molecular Biology, vol. 1542. Humana Press, New York, NY, U.S.A.

Nguyen, L. T., Schmidt, H. A., von Haeseler, A., and Minh, B. Q. 2015. IQ-TREE: A fast and effective stochastic algorithm for estimating maximum-likelihood phylogenies. Mol. Biol. Evol. 32:268-274.

Ordonez, N., Seidl, M. F., Waalwijk, C., Drenth, A., Kilian, A., Thomma, B. P., Ploetz, R. C., and Kema, G. H. 2015. Worse comes to worst: Bananas and Panama disease—When plant and pathogen clones meet. PLoS Pathog. 11:e1005197.

Perincherry, L., Lalak-Kańczugowska, J., and Stępień, Ł. 2019. *Fusarium*-produced mycotoxins in plant-pathogen interactions. Toxins (Basel) 11: 664.

Quesada, T., Gopal, V., Cumbie, W. P., Eckert, A. J., Wegrzyn, J. L., Neale, D. B., Goldfarb, B., Huber, D. A., Casella, G., and Davis, J. M. 2010. Association mapping of quantitative disease resistance in a natural population of loblolly pine (*Pinus taeda* L.). Genetics 186:677-686.

Quesada, T., Lucas, S., Smith, K., and Smith, J. 2019. Response to temperature and virulence assessment of *Fusarium circinatum* isolates in the context of climate change. Forests 10:40.

Reynolds, H. T., Slot, J. C., Divon, H. H., Lysøe, E., Proctor, R. H., and Brown, D. W. 2017. Differential retention of gene functions in a secondary metabolite cluster. Mol. Biol. Evol. 34:2002-2015.

Seppey, M., Manni, M., and Zdobnov, E. M. 2019. BUSCO: Assessing genome assembly and annotation completeness. Pages 227-245 in: Gene Prediction. M. Kollmar, ed. Methods in Molecular Biology, vol. 1962. Humana Press, New York, NY, U.S.A.

Smit, A., Hubley, R., and Green, P. 2015. RepeatMasker Open-4.0 2013-2015. https://www.repeatmasker.org/

Sperschneider, J., Gardiner, D. M., Dodds, P. N., Tini, F., Covarelli, L., Singh, K. B., Manners, J. M., and Taylor, J. M. 2016. EffectorP: Predicting fungal effector proteins from secretomes using machine learning. New Phytol. 210:743-761.

Stanke, M., Keller, O., Gunduz, I., Hayes, A., Waack, S., and Morgenstern, B. 2006. AUGUSTUS: Ab initio prediction of alternative transcripts. Nucleic Acids Res. 34:W435-W439.

Steenkamp, E. T., Rodas, C., Kvas, M., and Wingfield, M. J. 2012. *Fusarium circinatum* and pitch canker of *Pinus* in Colombia. Australas. Plant Pathol. 41:483-491.

Torres Bedoya, E., Bebber, D. P., and Studholme, D. J. 2021. Taxonomic revision of the banana Fusarium wilt TR4 pathogen is premature. Phytopathology 111:2141-2145.

Tsavkelova, E. A., Bömke, C., Netrusov, A. I., Weiner, J., and Tudzynski, B. 2008. Production of gibberellic acids by an orchid-associated Fusarium proliferatum strain. Fungal Genet. Biol. 45:1393-1403.

Vaillancourt, B., and Buell, C. R. 2019. High molecular weight DNA isolation method from diverse plant species for use with Oxford Nanopore sequencing. BioRxiv 783159. https://www.biorxiv.org/content/10.1101/783159v2

van Wyk, S., Harrison, C. H., Wingfield, B. D., De Vos, L., van der Merwe, N. A., and Steenkamp, E. T. 2019a. The RIPper, a web-based tool for genome-wide quantification of repeat-induced point (RIP) mutations. PeerJ 7:e7447.

van Wyk, S., Wingfield, B. D., De Vos, L., van der Merwe, N. A., Santana, Q. C., and Steenkamp, E. T. 2019b. Repeat-induced point mutations drive divergence between *Fusarium circinatum* and its close relatives. Pathogens 8:298.

Vaser, R., Sović, I., Nagarajan, N., and Šikić, M. 2017. Fast and accurate de novo genome assembly from long uncorrected reads. Genome Res. 27:737-746.

Venkatesh, N., and Keller, N. P. 2019. Mycotoxins in conversation with bacteria and fungi. Front. Microbiol. 10:403.

Walker, B. J., Abeel, T., Shea, T., Priest, M., Abouelliel, A., Sakthikumar, S., Cuomo, C. A., Zeng, Q., Wortman, J., Young, S. K., and Earl, A. M. 2014. Pilon: An integrated tool for comprehensive microbial variant detection and genome assembly improvement. PLoS One 9:e112963.

Walkowiak, S., Rowland, O., Rodrigue, N., and Subramaniam, R. 2016. Whole genome sequencing and comparative genomics of closely related Fusarium head blight fungi: *Fusarium graminearum, F. meridionale* and *F. asiaticum*. BMC Genomics 17:1014.

Wang, B., Yu, H., Jia, Y., Dong, Q., Steinberg, C., Alabouvette, C., Edel-Hermann, V., Kistler, H. C., Ye, K., Ma, L.-J., and Guo, L. 2020. Chromosome-scale genome assembly of *Fusarium oxysporum* strain Fo47, a fungal endophyte and biocontrol agent. Mol. Plant-Microbe Interact. 33:1108-1111.

Wiemann, P., Sieber, C. M., von Bargen, K. W., Studt, L., Niehaus, E.-M., Espino, J. J., Huß, K., Michielse, C. B., Albermann, S., Wagner, D., Bergner, S. V., Connolly, L. R., Fischer, A., Reuter, G., Kleigrewe, K., Bald, T., Wingfield, B. D., Ophir, R., Freeman, S., Hippler, M., Smith, K. M., Brown, D. W., Proctor, R. H., Münsterkötter, M., Freitag, M., Humpf, H. U., Güldener, U., and Tudzynski, B. 2013. Deciphering the cryptic genome: Genome-wide analyses of the rice pathogen *Fusarium fujikuroi* reveal complex regulation of secondary metabolism and novel metabolites. PLoS Pathog. 9:e1003475.

Wight, W. D., Kim, K. H., Lawrence, C. B., and Walton, J. D. 2009. Biosynthesis and role in virulence of the histone deacetylase inhibitor depudecin from *Alternaria brassicicola*. Mol. Plant-Microbe Interact. 22: 1258-1267.

Wikler, K., and Gordon, T. R. 2000. An initial assessment of genetic relationships among populations of *Fusarium circinatum* in different parts of the world. Can. J. Bot. 78:709-717.

Wingfield, B. D., Steenkamp, E. T., Santana, Q. C., Coetzee, M. P. A., Bam, S., Barnes, I., Beukes, C. W., Chan, W. Y., De Vos, L., Fourie, G., Friend, M., Herron, D. A., Kvas, M., Martin, S. H., Mlonyeni, X. O., Naidoo, K., Phasha, M. M., Postma, A., Reva, O., Roos, H., Simpson, M., Slippers, B., Sutherland, R., Van der Merwe, N. A., Van der Nest, M. A., Venter, S. N., Wilken, P. M., Zipfel, R., Wingfield, M. J., Gordon, T. R., Korf, I., Slinski, S., Holt, C., and Yandell, M. 2012. First fungal genome sequence from Africa: A preliminary analysis. S. Afr. J. Sci. 108:1-9.

Wingfield, M., Hammerbacher, A., Ganley, R., Steenkamp, E., Gordon, T., Wingfield, B., and Coutinho, T. 2008. Pitch canker caused by *Fusarium circinatum*—A growing threat to pine plantations and forests worldwide. Australas. Plant Pathol. 37:319-334.

Xu, M., Gao, X., Chen, J., Yin, Z., Feng, H., and Huang, L. 2018. The feruloyl esterase genes are required for full pathogenicity of the apple tree canker pathogen *Valsa mali*. Mol. Plant Pathol. 19:1353-1363.

Young, C., Minton, B., and Bronson, J. 2006. Resistance Screening Center Procedures Manual: A guide used in the operational screening of pines for resistance to pitch canker disease. United States Department of Agriculture, Southern Region, Forest Health Protection.

Zhang, H., Yohe, T., Huang, L., Entwistle, S., Wu, P., Yang, Z., Busk, P. K., Xu, Y., and Yin, Y. 2018. dbCAN2: A meta server for automated carbohydrate-active enzyme annotation. Nucleic Acids Res. 46: W95-W101.

Zhang, Y., Yang, H., Turra, D., Zhou, S., Ayhan, D. H., DeIulio, G. A., Guo, L., Broz, K., Wiederhold, N., Coleman, J. J., Donnell, K. O., Youngster, I., McAdam, A. J., Savinov, S., Shea, T., Young, S., Zeng, Q., Rep, M., Pearlman, E., Schwartz, D. C., Di Pietro, A., Kistler, H. C., and Ma, L. J. 2020. The genome of opportunistic fungal pathogen *Fusarium oxysporum* carries a unique set of lineage-specific chromosomes. Commun. Biol. 3:50.